BILINGUAL PUBLISHING CO.
Pioneer of Global Academics Since 1984

Journal of Marine Science
http://ojs.bilpublishing.com/index.php/jms

ARTICLE

Hydrocarbon Detection Based on Phase Decomposition in Chaoshan Depression, Northern South China Sea

Guangjian Zhong[1,2*] Renqi Jiang[3] Hai Yi[1,2] Jincai Wu[3] Changmao Feng[1,2] Gang Zhou[3] Kun Wang[3] Lina Liu[3] Ming Sun[1,2]

1. Key Laboratory of Marine Mineral Resources, Ministry of Natural Resources, Guangzhou, China
2. Guangzhou Marine Geological Survey, Guangzhou, Guangdong, China
3. New Horizons Ltd., Beijing, China

ARTICLE INFO

Article history
Received: 7 April 2021
Accepted: 19 April 2021
Published Online: 23 April 2021

Keywords:
Chaoshan Depression
South China sea
Amplitude attribute of -90° phase component
Hydrocarbon detection

ABSTRACT

Located in the northern South China Sea, Chaoshan Depression is mainly a residual Mesozoic depression, with a construction of Meso-Cenozoic strata over 7000m thick and good hydrocarbon accumulation conditions. Amplitude attribute of -90°phase component derived by phase decomposition is employed to detect Hydrocarbon in the zone of interest (ZOI) in Chaoshan Depression. And it is found that there are evident amplitude anomalies occurring around ZOI. Phase decomposition is applied to forward modeling results of the ZOI, and high amplitudes occur on the -90°phase component more or less when ZOI is charged with hydrocarbon, which shows that the amplitude abnormality in ZOI is probably caused by oil and gas accumulation.

1. Introduction

Chaoshan Depression is located in the northern South China Sea (Figure 1). The geological study of this depression began in the early 1990s, and it was found that the lower tectonic layers were Mesozoic marine sediments, with the largest thickness of about 7000m, which has the potential to generate hydrocarbons and the conditions to form various types of oil and gas traps [1-13]. Chaoshan Depression is a residual Mesozoic depression, which experienced mid-late Jurassic subsidence, late Jurassic to early Cretaceous uplift, superimposed burial of early to late Cretaceous, and then late Cretaceous Uplift and erosion. The Guangzhou Marine Geological Survey Bureau divided the Chaoshan Depression into five secondary tectonic units, namely Eastern Sag, Western Sag, Central Low Uplift, Northern Slope, Central Slope and Western Slope. Among them, ZOI in Central Low Uplift is selected as a favorable exploration target (Figure 1). This article will elaborate on petroleum potential and hydrocarbon detec-

**Corresponding Author:*
Guangjian Zhong,
Key Laboratory of Marine Mineral Resources, Ministry of Natural Resources; Guangzhou Marine Geological Survey, Guangzhou, China;
Email: 2645078906@qq.com
Funding:
Supported by "Investigation of Mesozoic Oil and Gas Resources in Northeast of the South China Sea, Project No. DD20190212" from China Geological Survey.

DOI: https://doi.org/10.30564/jms.v3i2.3063

tion analysis of the target.

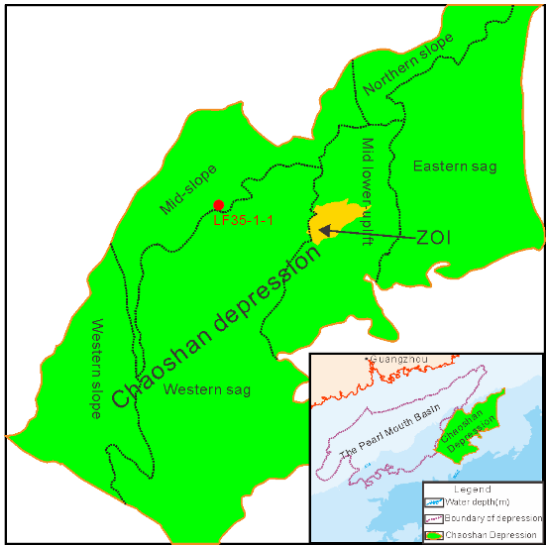

Figure 1. the location map of ZOI in Chaoshan Depression

Due to the shortage of available drilling data, reliable petrophysical data and hydrocarbon information in the target area of the Chaoshan Depression (Figure1), there is a large uncertainty in the direct prediction of oil and gas with conventional techniques. In order to make a breakthrough to the situation of Mesozoic oil and gas exploration in the Chaoshan Depression, this study applies phase decomposition amplitude attribute analysis techniques for direct hydrocarbon detection.

2. Petroleum Geology Conditions in Chaoshan Depression

Well LF35-1-1 confirmed that Chaoshan Depression is filled with Cretaceous continental sediments and Middle-Late Jurassic marine sediments, among which Middle-Late Jurassic marine sediments have good petroleum geological conditions [14-15].

2.1 Source Rocks

The upper part of the Middle-Upper Jurassic strata revealed by well LF35-1-1 is composed of gray-black veined layered mudstone, argillaceous siltstone with siliceous rock, containing a small amount of micrite limestone; the lower part is gray-black veined layered mudstone and shaly siltstone with sandstone, limestone. The mudstones are rich in organic debris. A set of river-lake sediments is generally made up of the Cretaceous strata. The upper part is a combination of purple mudstone, siltstone and sandstone with a small amount of marl, and the lower part is a combination of gray grained layered mudstone, siltstone and sandstone, containing some organic debris (Table 1).

2.2 Reservoir Conditions

According to the formations revealed by well LF35-1-1 and seismic data interpretation, there may be two sets of reservoirs in the Chaoshan Depression. One set is the river-lake sandstone reservoir in Cretaceous, and the other set is coastal-shallow sea sandstone, slope fan and basin-bottom fan sandstone in the Upper-mid Jurassic, and sandstone and limestone reservoirs in transgressive system tracts.

The seismic profile (Figure 2) across ZOI shows that a set of limestone layers with stable thickness are distributed on the top of the Middle Jurassic (T_{j2} interface). A set of submarine fan sandstones advancing from SE to NW are developed on the top of the Upper Jurassic. The fan

Table 1. Dark mud-rock properties at well LF35-1-1

Interval (m)	Strata	Thickness	Lithology	Paleo-strata thickness	Effective source rock thickness	TOC(%)		Evaluation
						Min-max	Average (Number of samples)	
977-1369	K	392	Dark mud-rock	0	0	0.05-0.54	0.10(25)	Non-source
			Tuff	33	0	0.06-0.30	0.15(6)	Non-source
1369-1698	K	329	Dark sandy mud-rock	45.5	0	0.06-0.11	0.08(15)	Non-source
			Tuff	215	0	0.14-0.63	0.27(28)	Non-source
1698-2412	J2+3	713	Dark sandy mud-rock	529.38 (with tuff and sandstone reduced)	82.87	0.5-1.15	0.70(36)	Poor-moderate source
					46.16	1-1.48	1.32(11)	Moderate to good source

 DOI: https://doi.org/10.30564/jms.v3i2.3063

root (inner fan and levee deposits) is located on southeast of the profile. And mid-fan mainly develops in middle and northwest with mid-fan channel deposits, where there are sandstone reservoirs of the best properties. Mid-fan frontal deposits develop in northwest.

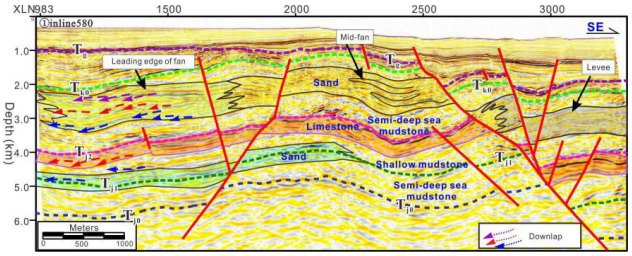

Figure 2. seismic facies interpretation profile for reservoirs of ZOI

2.3 Seal Conditions

According to well LF35-1-1, multiple layers of mudstones encountered in this well are thick, and the maximum thickness of an individual layer is more than 30 m. They should have good sealing capabilities and serve as important regional cap rocks in the area. In addition, there are many sets of mudstones in the Middle-Upper Jurassic, and these mudstones are mostly characteristics of continuous or poorly continuous, medium or weak amplitude reflections on the seismic profile. According to the seismic profile, the distribution of these strata is stable, which can also serve as a regional cap rock.

3. Amplitude Attribute of -90° Phase Component by Phase Decomposition

Phase decomposition is a unique and creative technology for hydrocarbon detection, originated by Castagna [17]. The acoustic impedance variations caused by pore fluids or lithology changes do not always produce very obvious amplitude anomalies on conventional post-stack profiles. By decomposing seismic traces into different phase components and suppressing unwanted phase components, it is possible to identify some subtle hydrocarbon, lithological changes or anomalous responses caused by sand channels, where significant amplitude anomalies occur at the expected phase components. This technology has become a very effective tool for special geological body identification and hydrocarbon detection [18-19].

Based on spectral decomposition [20], any seismic trace can be decomposed into 2D functions, amplitude spectrum and phase spectrum. A seismic trace S (t) is a 1D function whose amplitude varies with time. The amplitude spectrum A (f, t) is a 2D function whose amplitude varies with both time and frequency, and the phase spectrum θ (f, t) is a 2D function whose phase varies with time and frequency also. If we combine the amplitude spectrum and the phase spectrum into a function A (f, t) * cosθ (f, t), then a two-dimensional function representing reflection amplitude changes with phase and time can be obtained by the following formula:

$$S'(\theta,t)=\int_{f_1}^{f_2} A(f,t)\cos\theta(f,t)df \quad (1)$$

Where f1 and f2 are the starting and ending frequencies of the band. We define this function as phase gather. Any desired phase component in the specified frequency band is extracted as follows:

$$S'(t)=\int_{\theta_1}^{\theta_2} S'(\theta,t)d\theta \quad (2)$$

Where θ1 and θ2 are the starting and ending phases of the phase band. In this way, the seismic reflection events with specific spectral characteristics can be suppressed or enhanced. The process of decomposing a seismic trace into a two-dimensional function of amplitude with time and phase is called phase decomposition. The amplitude change with time at a specific phase is referred to as a phase component. The seismic reflections caused by small impedance changes in the layer below the tuning thickness can be amplified, making specific geological features easier to discover. Any pair of reflection coefficients can be expressed as the sum of an odd and an even component. The reflection coefficients of even component are the same in size and sign, and those of odd component are the same in size and opposite in sign (17). As to an individual thin layer, the impedance variation changes the reflectivity of odd component, and thus the phase of the local reflectivity, while the even component remains almost unchanged. A phase filter can be designed and applied to seismic data based on the method described above, and the odd component may show an obviously strong amplitude anomaly at the location where weak amplitude appears originally. Especially in the case of low-impedance thin gas or light oil sands (bright spots), the amplitude abnormality corresponding to gas saturation will appear in the -90° phase component. Therefore, in practical applications, amplitude attribute analysis of -90° phase component is often used as a means for hydrocarbon detection.

4. Forward Modeling Analysis of Hydrocarbon Detection in Chaoshan Depression

-90° phase component technology for hydrocarbon detection has achieved excellent results in practical applications. In the exploration target area of Chaoshan Depression, there is no well drilled available. It is wondered

DOI: https://doi.org/10.30564/jms.v3i2.3063

that the technique of phase decomposition and -90° phase component hydrocarbon detection can achieve good results. We conduct forward modeling using the reservoir properties adjacent to the Chaoshan Depression to see what will happen to the amplitude attribute of -90° phase component if target reservoir contains oil and gas, and whether it can predict oil and gas.

4.1 Model Establishment

The main purpose of establishing the forward model is to investigate the response characteristics of the amplitude of the -90° phase component to oil, gas or brine. The forward modeling is implemented using Leonardo technology and then the response characteristics of the two attributes with different pore fluids are summarized.

In practical work, there are three types of impedance changes for reservoir and its surrounding rocks: ① The impedance of surrounding rocks is higher than that of oil, gas or brine reservoirs, and oil-gas reservoirs are characteristics of bright spots; ② The impedance of surrounding rock is lower than that of oil, gas or brine reservoirs, and oil-gas reservoirs is characteristics of dim spots; ③ The impedance of surrounding rock is lower than that of brine-bearing reservoirs, but higher than that of oil-gas reservoirs, which shows polarity reversal (Figure 3).

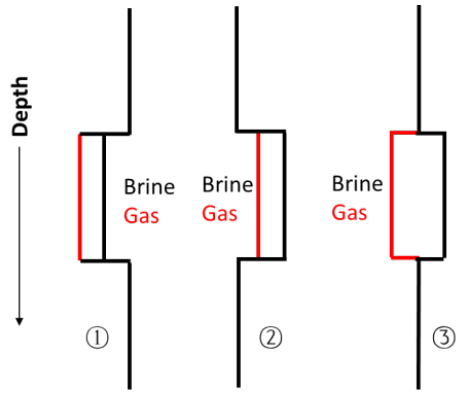

Figure 3. Assemblage patterns of reservoir and surrounding rocks

According to the above assemblage patterns for reservoir and the surrounding rocks, and the drilling data of well LF35-1-1 in northern slope, the geological model is established firstly according to the lithology combination and velocity changes in the target area. The upper Jurassic stratum is the target zone, with a depth of about 1700-2300 meters. The lithology of the overlying rocks includes siliceous rock, mudstone, and argillaceous siltstone; and the reservoir lithology includes sandstone, siltstone; and underlying rocks are limestone. Various lithology and its velocity are as follows in Table 2.

Table 2. rock types and their velocities listed

Lithology	Depth(m)	Velocity(m/s)
Siliceous rock	1700-1900	5350
Mudrock	1950-2080	4200
Shaly siltstone and siltstone	1900-1950 2080-2200	5250
Limestone	2200-2300	5450

According to the velocity characteristics of siliceous rock and mudstone, the following three models are established (Figure 4-6). For No. 1 model, the overlying rock is siliceous rock with velocity of 5350m/s, which is greater than that of the sandstone reservoir. For No. 2 model, the overlying rock is mudstone, and its velocity of 4200 m/s is less than that of sandstone reservoir. As to No. 3 model, the overlying rock is a combination of siliceous and mudstone with the velocity of 5100m/s, which is the average velocity of siliceous rocks and mudstones, and the caprock velocity are close to that of the sandstone reservoir.

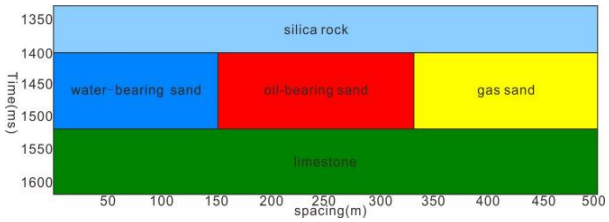

Figure 4. No. 1 model

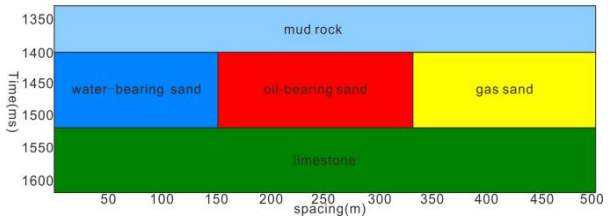

Figure 5. No. 2 model

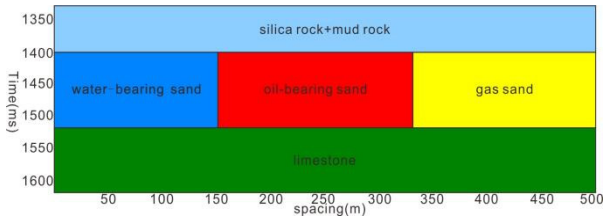

Figure 6. No. 3 model

4.2 Seismic Modeling in Chaoshan Depression

The forward seismic profiles corresponding to the three models are displayed in Figures7-9. According to the synthetic profiles by forward modeling, the reservoir top of

DOI: https://doi.org/10.30564/jms.v3i2.3063

model 1 is a trough, and the amplitude of oil/gas-bearing case is significantly higher than the brine-bearing reservoir. The reservoir top of model 2 is a peak reflection, and the amplitude when oil/gas-bearing case is significantly lower than brine-bearing case reservoir. The brine layer top of model 3 is a peak reflection, and the gas layer is a trough. The amplitude of the brine layer is slightly different from the gas layer, and the oil layer is a peak of weak amplitude. On seismic sections, it difficult to directly identify the oil and gas layer.

The amplitude attribute of the -90° phase component is extracted on forward synthetic seismic data (Figure 10-12). On -90° phase component profiles, it is similar that the gas layer has the strongest amplitude and brine layer the weakest amplitude, and the oil layer amplitude between gas and brine.

In Table 2, the absolute amplitude values of synthetic seismic data and -90° phase attributes are read from the three models of brine, oil and gas respectively. And amplitude values of -90° phase attributes are cross-plotted against those of synthetic seismic data (Figure 13). On the cross-plotting, there is not a uniform threshold to identify oil and gas layers for original synthetic seismic amplitude only, while for -90° phase amplitudes, uniform thresholds can be seen between brine and oil and gas. The amplitude value above 0.0005 is gas layer, and the amplitude between 0.0035-0.0005 oil layer, and the amplitude less than 0.00035 brine layer.

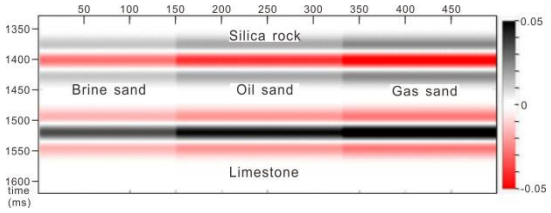

Figure 7. Synthetic section of model 1

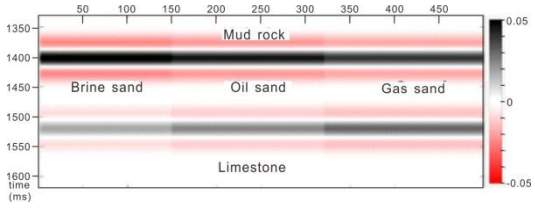

Figure 8. Synthetic section of model 2

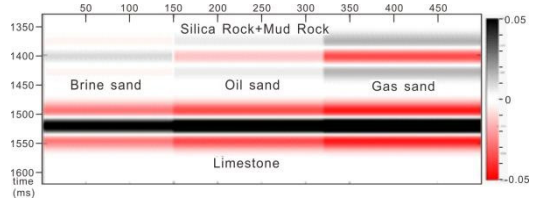

Figure 9. Synthetic section of model 3

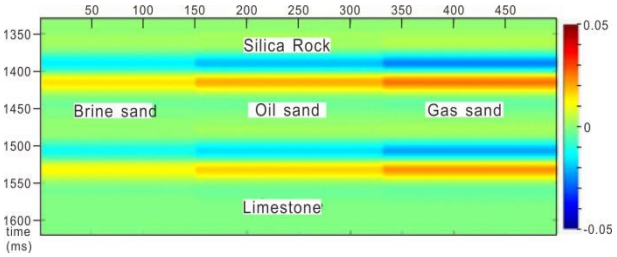

Figure 10. model 1

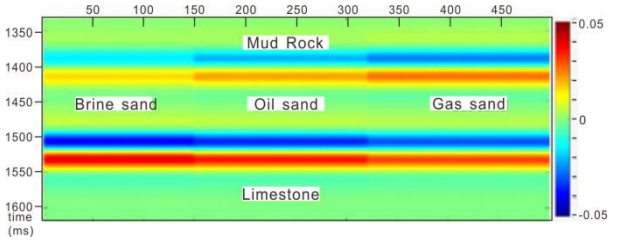

Figure 11. model 2

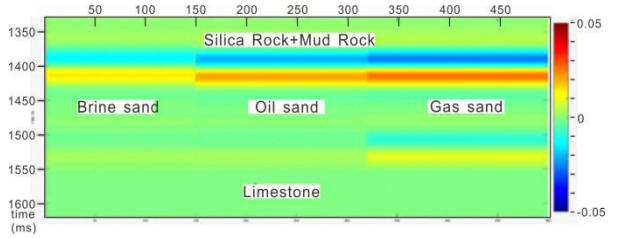

Figure 12. model 3

Table 2. Synthetic amplitudes and its phase component for different pore fluids cases

Model	Fluids	Absolute amplitude of synthetic data	Absolute amplitude of -90° phase component
No. 1	Gas	0.053	0.00051
	Oil	0.041	0.00041
	Water	0.028	0.00031
No. 2	Gas	0.078	0.00052
	Oil	0.092	0.00042
	Water	0.11	0.00032
No. 3	Gas	0.021	0.00052
	Oil	0.0078	0.00043
	Water	0.0052	0.00028

DOI: https://doi.org/10.30564/jms.v3i2.3063

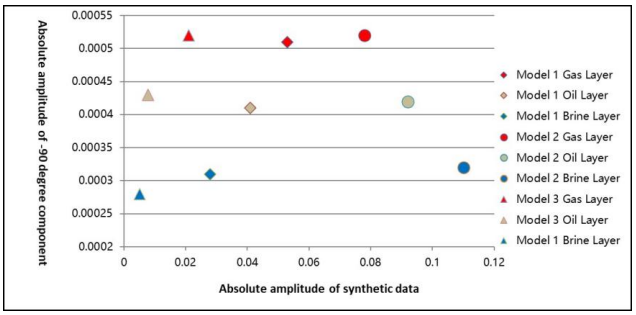

Figure 13. Cross plotting for synthetic amplitudes and its phase component of 3 models

5. Identification of Exploration Targets in Chaoshan Depression

Well LF35-1-1 confirms that there are two sets of reservoir-cap rock assemblages in the Chaoshan Depression. One is interbedded sandstone and mudstone in Cretaceous, and the other is the Middle-Upper Jurassic. And the latter is the main target interval for oil and gas exploration. For this main exploration target, the reservoir occurrence is analyzed by extracting conventional seismic amplitude attributes. Hydrocarbon detection is performed using -90° phase component amplitude attribute analysis and spectrum decomposition peak amplitude attribute analysis respectively, so as to verify the two prediction results mutually and increase hydrocarbon detection confidence.

5.1 Analysis of Conventional Seismic Amplitude Attributes

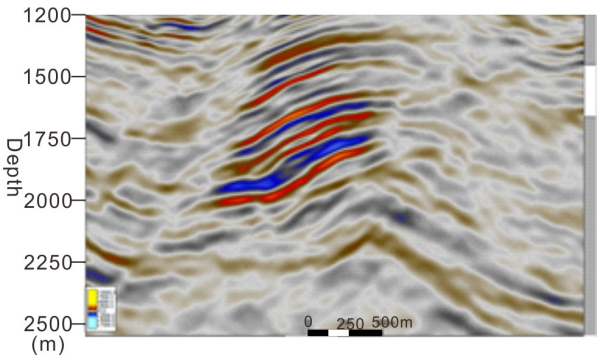

Figure 14. Original seismic section around ZOI

Seismic amplitude attributes can indicate reservoir property variations to a certain extent, so the seismic amplitude attributes are usually applied to qualitatively analyze reservoir development. The seismic section along one favorable exploration target in the Chaoshan Depression is shown in Figure 14. On the section, the ZOI of Upper Jurassic shows strong reflections locally, which is probably the seismic response of the reservoir with better properties. By extracting its amplitude attribute, the lateral distribution range of the strong reflection of ZOI is preliminarily delineated, which probably corresponds to the range of favorable reservoirs of ZOI (Figure 15).

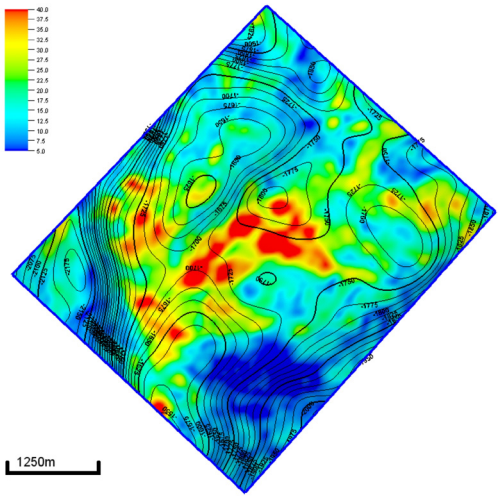

Figure 15. Original seismic amplitude attribute map extracted along ZOI

5.2 -90° Phase Component Amplitude Attribute Analysis for Hydrocarbon Detection

The -90° phase component amplitude attribute by phase decomposition is used to study on the seismic section where there are strong reflections around ZOI, to clarify the distribution of abnormal amplitudes of the -90° phase component attribute, and then to identify its possible oil and gas distribution scope.

A comparison between the original seismic profile and the -90° phase component profile is illustrated in Figure 16. From this comparison, strong amplitude reflections on the -90° phase component profile do not coincide with all those on the conventional seismic profile, and some strong amplitudes are no longer strong on -90° phase component profile. According to the previous forward modeling results, strong amplitudes on the -90° phase component profile is probably caused by presence of oil and gas. By extracting the amplitude attribute of the -90° phase component, the possible oil and gas distribution range is identified in Figure 17 on the right.

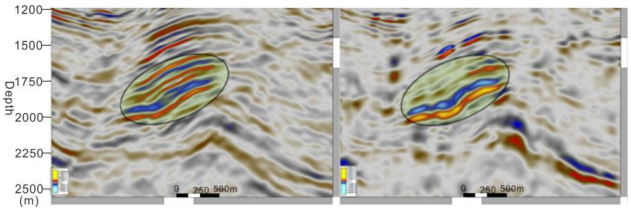

Figure 16. the seismic section (left) and -90° phase component section (right) of Up-Jurassic reservoir

DOI: https://doi.org/10.30564/jms.v3i2.3063

The comparison between the attribute map of conventional amplitude and that of -90° phase component along ZOI is illustrated in Figure 17. There are clusters of strong amplitude characteristics on both maps. However, the strong amplitude range on the -90-degree phase component map is reduced, and the boundary of the strong amplitude range is clearer, and it is more consistent structural contours. Obviously stronger amplitudes of -90-degree phase component especially occur on structural highs (Figure 17b). Therefore, it is speculated that the oil and gas accumulation is extremely likely to occur in the areas with high amplitudes.

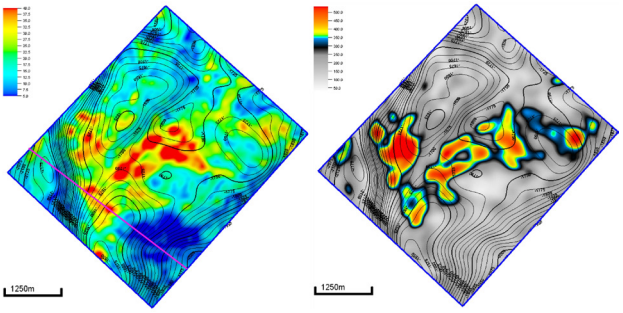

Figure 17. The attribute map (left) and -90° phase component map (right) of Up-Jurassic reservoir

6. Conclusions

For exploration frontier areas under study, there is much uncertainty to apply conventional seismic attribute analysis for identifying oil and gas prospective targets due to few wells available. Fortunately, the joint application of this method, -90° phase component amplitude attribute analysis by phase decomposition is an effective alternative in these areas. Together with its forward modeling analysis, -90° phase component amplitude attribute analysis method is used to predict reservoir oil and gas bearing property of the ZOI in Chaoshan Depression, which indicates that there are probably oil-bearing layers in Upper Jurassic reservoirs.

References

[1] Liu G D. 2001. The second exploitation of the oil and gas resources in China [J]. Progress in Geophysics, 16(4):1-3.

[2] Zhang J Y, SUN Z, Zhang S F. 2014. Analysis of Mesozoic tectonic deformation in the Chaoshan Depression of Pearl River Mouth Basin [J]. Journal of Tropical Oceanography, 33(5):41-49.

[3] Hao H J, Lin H M, Yang M X, et al. 2001. The Mesozoic in Chaoshan depression: A new domain of petroleum exploration. China Offshore Oil and Gas (in Chinese), 15(3):157-163.

[4] Wang L L, Cheng R H, LI F, et al. 2009. The Mesozoic Sedimentary Sequences, Correlation and Geological Significance for Petroleum of the North Margin of South China Sea [J]. Journal of Jilin University (Earth Science Edition), 39(2):175-182.

[5] Zhang L, Geng A s, Wang LL, et al. 2012. Assessment of Mesozoic source rocks at The Margin of South China Continent [J]. Marine Geology & Quaternary Geology, 32(1):99-108.

[6] Ji Z Y, Zhao H Q, et al. 2014. The Mesozoic Petroleum System of Chaoshan depression. Petroleum Geology and Enginerering, 28(3): 9-15.

[7] Wang P, Xia K Y, Huang C L. 2000. The Mesozoic Marine sediment distribution and Geology-Geophysics characteristic at the North-Eastern of South China Continent [J]. Journal of Tropical Oceanography, 19(4):28-35.

[8] Duan J C, Mi H F. 2012. Seismic Facies and Sedimentary Facies study of Mesozoic in Chaoshan Sag [J]. Resources & Industries, 14(1):100-105.

[9] Hao H J, Wang R L, Zhang X T, et al. 2004. Mesozoic marine sediment identification and distribution in the eastern Pearl River Mouth Basin. China Offshore Oil and Gas, 16(2):84-88.

[10] Zhang Q L, Zhang H F, Zhang X T, et al. 2018. The upper Cretaceous prototype basin of the Chaoshan depression in the northern South China Sea and its tectonic setting [J].Chinese Journal of Geophysics,vol61(10):p4308-4321.

[11] Zhou D, Chen H Z. Sun Z, et al. 2005. Three Mesozoic sea basins in the eastern and southern South China Sea and their relation to Tethys and Paleo-Pacific domains. Journal of Tropical Oceanography, 24(2):16-25.

[12] Yao B C, Zhang L, Wei Z Q, et al. 2011. The Mesozoic Tectonic Characteristics and Sediment Basins in the Eastern Margin of South China Continen [J]. Marine Geology & Quaternary Geology, 31(3):47-60.

[13] Zhong G J, Wu S M, Feng C M. 2011. Sedimentary model of Mesozoic in the northern South China Sea. Journal of Tropical Oceanography, 30(1):43-48.

[14] Hao H J, Shi H S, Zhang X T, et al. 2009. Mesozoic sediments and their petroleum geology conditions in Chaoshan sag: A discussion based on drilling results from the exploratory well LF35-1-1. China Offshore Oil and Gas (in Chinese), 21(3):151-156.

[15] Zhong G J, Yi H, Lin Z, et al. 2007. Characteristic of Source Rocks and Mesozoic in Continental Slope Area of Northeastern the South China Sea and East Guangdong of China. XINJIANG Petroleum Geology, 28 (6):676-680.

[16] Yang S C, Tong Z G, He Q, et al. 2009. Mesozoic hydrocarbon generation history and igneous intrusion

DOI: https://doi.org/10.30564/jms.v3i2.3063

impacts in Chaoshan depression, South China Sea: A case of LF35-1-1 well. China Offshore Oil and Gas (in Chinese), 20(3):152-156.

[17] Castagna, J., A. Oyem, O. Portniaguine, and U. Aikulola, 2016, Phase decomposition: Interpretation, 4, no. 3, SN1–SN10,
DOI: 10.1190/INT-2015-0150.1.

[18] Elita Selmara De Abreu, John Patrick Castagna and Gabriel Gil, 2018, Case study: Phase-component amplitude variation with angle: Geophysics, 84, B285–B297,
DOI: 10.1190/GEO2018-0762.1.

[19] Barbato, U., O. Portniaguine, B. Winkelman, and J. Castagna, 2017, Phasedecomposition as a DHI in bright-spot regimes: A Gulf of Mexico casestudy: 87th Annual International Meeting, SEG, Expanded Abstracts, 3976-3980,
DOI: 10.1190/segam2017-17737608.1.

[20] Partyka, G., J. Gridley, and J. Lopez, 1999, Interpretational applications ofspectral decomposition in reservoir characterization: The Leading Edge, 18, 353-360.

[21] Barnes, A. E., 1993, Instantaneous spectral bandwidth and dominantfrequency with applications to seismic reflection data: Geophysics, 58,419-428,
DOI: 10.1190/1.1443425.

[22] Bracewell, R. N., 1978, The Fourier Transform and its applications: McGraw-Hill.

 DOI: https://doi.org/10.30564/jms.v3i2.3063